International Journal of Microwave and Wireless Technologies

cambridge.org/mrf

Analytical solution of higher order modes of a dielectric-lined eccentric coaxial cable

Mehdi Gholizadeh and Farrokh Hojjat Kashani

Department of Electrical Engineering, Iran University of Science & Technology, Narmak, Tehran, Iran

Research Paper

Cite this article: Gholizadeh M, Hojjat Kashani F (2021). Analytical solution of higher order modes of a dielectric-lined eccentric coaxial cable. *International Journal of Microwave and Wireless Technologies* **13**, 247–254. https://doi.org/10.1017/S1759078720000926

Received: 29 February 2020
Revised: 17 June 2020
Accepted: 18 June 2020
First published online: 15 July 2020

Keywords:
Analytical Solution; Hybrid Modes; Cutoff Frequencies; Dielectric-Lined Eccentric Coaxial Cable

Author for correspondence:
Mehdi Gholizadeh, E-mail: mehdi.gholizadeh1991127@gmail.com

Abstract

This study provides an analytic method for the calculation of the cutoff frequencies and waveguide modes of a partially filled eccentric coaxial cable. The method is based on the expressions of the involved electromagnetic fields in bipolar coordinate systems and the validity range of the solution is discussed. It is shown how the waveguide geometry and dielectric parameters may be selected to engineer the lined waveguide's spectral response. Numerical results are included which show good agreement with the corresponding results from full-wave simulations by commercial software.

Introduction

Without modifying the dimension of conductors, the characteristic impedance of a coaxial cable is adjustable by laterally changing the offset of the inner conductor. This technique can be used to realize a quarter-wave matching element that forms one of the sections in a multisection quarter-wave transformer for broadband-matching applications [1]. Besides, the analysis of cavities excited by thin probes can be simplified using eccentric circular metallic waveguide structures with a small ratio of inner-to-outer conductor dimensions [2]. Despite of these interesting applications, the shape of boundaries severely limits the possibility for analytical solutions of eccentric circular metallic waveguide configurations [3, 4]. The investigations of this type of waveguide have initiated interest of researchers for a long time [1–15]. Various techniques have been used to obtain numerical results: point-matching [5], conformal transformation [6], related addition theorem [7], a combination of the conformal mapping of the cross-section with the intermediate problems method to obtain the lower bounds for the cutoff frequencies and the Rayleigh–Ritz method for the upper bounds [8], perturbation techniques [2], transforming eccentric coaxial into coaxial configuration using bilinear transformation [9], a combination of the polynomial approximation and quadratic functions with the Rayleigh–Ritz [10], a combination of conformal mapping with the finite-element [11], a combination of conformal mapping with the finite-difference [1, 12, 13], a combination of the fundamental solutions and particular solutions methods [14], a combination of the perturbation method with the separation of variables' technique followed by the well-known cosine and sine laws [3], and the separation of variables' technique in bipolar coordinate systems (BCSs) [15]. All these investigations have been concentrated on the evaluation of the higher-order modes and their cutoff frequencies without any dielectric support between the inner and outer conductors. In [16], eccentric circular metallic waveguide supported by dielectric slab between the inner and outer conductors has been investigated using the finite element approach. Propagation in composite cylindrical structures, composed of a bianisotropic cylinder embedded in an unbounded bianisotropic space and enclosing an array of parallel bianisotropic rods, has been studied in [17]. In [18], higher order modes of two wire waveguides have been investigated using BCS and separation of variable technique.

This paper presents an analytical solution of higher order modes in a dielectric-lined eccentric circular metallic waveguide. In [15], the solution of the Helmholtz equation in BCS has been obtained using the technique of separation of variables and the validity range of the solution has been discussed. In this study, this solution has been applied to analyze the higher order modes of a dielectric-lined eccentric circular metallic waveguide. Rather than TE and TM modes, this structure also supports hybrid electric (HE) and hybrid magnetic (EH) modes which are similar to the transversal TE and TM modes of a homogeneously filled eccentric coaxial cable, except that the longitudinal electric and magnetic fields do not generally vanish. The cutoff frequencies of the higher order modes (TE, TM, HE, and EH modes in this case) have been determined by enforcing the boundary conditions and the continuity of the tangential electric- and magnetic-field components at the boundaries of the structure and an analytical expression is proposed for the electromagnetic fields. Moreover, it will be shown that this approach significantly works better than the method presented in [15] in calculating the cutoff frequencies of a homogeneously filled eccentric circular metallic waveguide. The paper is organized as follows. Section "Problem formulation and solution" presents the

© Cambridge University Press and the European Microwave Association 2020

CAMBRIDGE UNIVERSITY PRESS

formulation of the problem. The obtained results are discussed in section "Results and discussion". Finally, section "Conclusion" concludes this research.

Problem formulation and solution

Figure 1 depicts the geometry of the partially filled eccentric coaxial line under consideration. A hollow infinite perfect electric conductor (PEC) cylinder of radius R_1 (the outer conductor) in the z-direction eccentrically surrounds a dielectric cylinder (of radius R_2 with permittivity $\varepsilon_2 = \varepsilon_{r2}\varepsilon_0$ and permeability $\mu_2 = \mu_{r2}\mu_0$) which itself eccentrically encloses another PEC cylinder of radius R_3 (the inner conductor). The remaining space inside the waveguide is filled by another dielectric material with permittivity $\varepsilon_1 = \varepsilon_{r1}\varepsilon_0$ and permeability $\mu_1 = \mu_{r1}\mu_0$. The offset of the inner dielectric cylinder (region 2) and the PEC core are denoted D_1 and D_2, respectively. This type of waveguide can be easily described using BCS. In this paper, it has been supposed the circles in Fig. 1 lie to the right of the y-axis ($0 \le \zeta < +\infty$). The relations between the parameters of BCS and the dimensions of the waveguide can be written as follows:

$$R_1 = \frac{a}{\sinh(\zeta_1)}, \quad R_2 = \frac{a}{\sinh(\zeta_2)}, \quad R_3 = \frac{a}{\sinh(\zeta_3)} \tag{1}$$

$$\begin{aligned} D_1 &= a(\coth(\zeta_1) - \coth(\zeta_2)), \\ D_2 &= a(\coth(\zeta_1) - \coth(\zeta_3)) \end{aligned} \tag{2}$$

where a is an arbitrary positive real number and $2a$ shows how far apart the poles ($P1(a, 0)$ and $P2(-a, 0)$) of the BCS lie. It is obvious that $\zeta = \zeta_1$, $\zeta = \zeta_2$, and $\zeta = \zeta_3$ determine the boundaries of the waveguide in BCS, where $\zeta_1 < \zeta_2 < \zeta_3$. The Helmholtz equation in BCS can be written as:

$$\frac{\partial^2\varphi(\zeta,\eta)}{\partial\zeta^2} + \frac{\partial^2\varphi(\zeta,\eta)}{\partial\eta^2} + \frac{a^2k_c^2\varphi(\zeta,\eta)}{(\cosh(\zeta) - \cos(\eta))^2} = 0. \tag{3}$$

and its solution is as follows:

$$\begin{aligned} \varphi(\zeta,\eta) &= \varphi_\zeta(\zeta)\varphi_\eta(\eta) = (A_1\sin(n\eta) + A_2\cos(n\eta)) \\ &(B_1J_n(2ak_ce^{-\zeta}) + B_2Y_n(2ak_ce^{-\zeta})), \quad |\zeta| \ge 3 \end{aligned} \tag{4}$$

where φ represents the scalar function that illustrates the longitudinal component of the field, n is the azimuthal mode index, A_1, A_2, B_1, and B_2 are the amplitude coefficients, $Jn(x)$ and $Yn(x)$ are the Bessel functions of order n of first and second kinds, respectively, $k_c^2 = k^2 - \gamma^2$, $k = \omega\sqrt{\mu\varepsilon}$, and γ is the axial propagation constant [15]. For the structure shown in Fig. 1, $|\zeta| \ge 3$ means $D_1/R_1 = 1$ or $D_2/R_1 = 1$. In other words, (4) is valid for either $D_1/R_1 = 1$ and every arbitrary value of D_2/R_1, or $D_2/R_1 = 1$ and every arbitrary value of D_1/R_1. By suppressing the propagation term ($e^{-\gamma z}$) and the time–harmonic nature of the fields ($e^{j\omega t}$), since the tangential electric-field components must vanish at the outer PEC boundary ($\zeta = \zeta_1$), the electric- and magnetic-field components in the z-direction in region 1 ($\zeta_1 \le \zeta \le \zeta_2$) can be written as:

$$E_{1z} = C_1F_{1n}(2ak_{1\zeta}e^{-\zeta})\cos(n\eta) \tag{5}$$

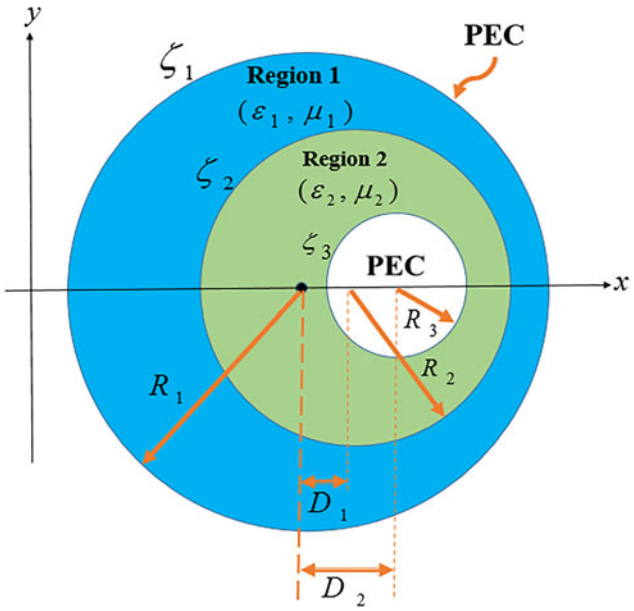


Fig. 1. Transverse cross-section of the partially filled eccentric coaxial cable.

$$H_{1z} = C_2G_{1n}(2ak_{1\zeta}e^{-\zeta})\sin(n\eta) \tag{6}$$

where

$$\begin{aligned} F_{1n}(2ak_{1\zeta}e^{-\zeta}) &= Y_n(2ak_{1\zeta}e^{-\zeta_1})J_n(2ak_{1\zeta}e^{-\zeta}) \\ &- J_n(2ak_{1\zeta}e^{-\zeta_1})Y_n(2ak_{1\zeta}e^{-\zeta}) \end{aligned} \tag{7}$$

$$\begin{aligned} G_{1n}(2ak_{1\zeta}e^{-\zeta}) &= Y'_n(2ak_{1\zeta}e^{-\zeta_1})J_n(2ak_{1\zeta}e^{-\zeta}) \\ &- J'_n(2ak_{1\zeta}e^{-\zeta_1})Y_n(2ak_{1\zeta}e^{-\zeta}) \end{aligned} \tag{8}$$

Here, C_1 and C_2 are the amplitude coefficients, $k_{1\zeta} = k_1^2 - \gamma^2$ and $k_1 = \omega\sqrt{\mu_1\varepsilon_1}$. Similarly, the solution in region 2 ($\zeta_2 \le \zeta \le \zeta_3$) has the following form:

$$E_{2z} = C_3F_{2n}(2ak_{2\zeta}e^{-\zeta})\cos(n\eta) \tag{9}$$

$$H_{2z} = C_4G_{2n}(2ak_{2\zeta}e^{-\zeta})\sin(n\eta) \tag{10}$$

where

$$\begin{aligned} F_{2n}(2ak_{2\zeta}e^{-\zeta}) &= Y_n(2ak_{2\zeta}e^{-\zeta_3})J_n(2ak_{2\zeta}e^{-\zeta}) \\ &- J_n(2ak_{2\zeta}e^{-\zeta_3})Y_n(2ak_{2\zeta}e^{-\zeta}) \end{aligned} \tag{11}$$

$$\begin{aligned} G_{2n}(2ak_{2\zeta}e^{-\zeta}) &= Y'_n(2ak_{2\zeta}e^{-\zeta_3})J_n(2ak_{2\zeta}e^{-\zeta}) \\ &- J'_n(2ak_{2\zeta}e^{-\zeta_3})Y_n(2ak_{2\zeta}e^{-\zeta}) \end{aligned} \tag{12}$$

Here, C_3 and C_4 are the amplitude coefficients, $k_{2\zeta} = k_2^2 - \gamma^2$ and $k_2 = \omega\sqrt{\mu_2\varepsilon_2}$. The other field components in each region can be

https://doi.org/10.1017/S1759078720000926 Published online by Cambridge University Press

extracted from the following equations:

$$E_\zeta = \frac{-\gamma}{hk_\zeta^2}\left(\frac{\partial E_z}{\partial \zeta} + \frac{j\omega\mu}{\gamma}\frac{\partial H_z}{\partial \eta}\right) \tag{13}$$

$$E_\eta = \frac{-\gamma}{hk_\zeta^2}\left(\frac{\partial E_z}{\partial \eta} - \frac{j\omega\mu}{\gamma}\frac{\partial H_z}{\partial \zeta}\right) \tag{14}$$

$$H_\zeta = \frac{-\gamma}{hk_\zeta^2}\left(\frac{\partial H_z}{\partial \zeta} - \frac{j\omega\varepsilon}{\gamma}\frac{\partial E_z}{\partial \eta}\right) \tag{15}$$

$$H_\eta = \frac{-\gamma}{hk_\zeta^2}\left(\frac{\partial H_z}{\partial \eta} + \frac{j\omega\varepsilon}{\gamma}\frac{\partial E_z}{\partial \zeta}\right) \tag{16}$$

where $h = a/(\cosh\zeta - \cos\eta)$ is the transversal scale factor.

Therefore, we can write the following relations for each region:

$$E_{1\zeta} = \frac{-\gamma}{hk_{1\zeta}^2}(-C_1 2ak_{1\zeta}e^{-\zeta}F'_{1n}(2ak_{1\zeta}e^{-\zeta}) + C_2\frac{nj\omega\mu_1}{\gamma}G_{1n}(2ak_{1\zeta}e^{-\zeta}))\cos(n\eta) \tag{17}$$

$$E_{1\eta} = \frac{-\gamma}{hk_{1\zeta}^2}(-C_1 nF_{1n}(2ak_{1\zeta}e^{-\zeta}) + C_2\frac{j\omega\mu_1}{\gamma}2ak_{1\zeta}e^{-\zeta}G'_{1n}(2ak_{1\zeta}e^{-\zeta}))\sin(n\eta) \tag{18}$$

$$E_{2\zeta} = \frac{-\gamma}{hk_{2\zeta}^2}(-C_3 2ak_{2\zeta}e^{-\zeta}F'_{2n}(2ak_{2\zeta}e^{-\zeta}) + C_4\frac{nj\omega\mu_2}{\gamma}G_{2n}(2ak_{2\zeta}e^{-\zeta}))\cos(n\eta) \tag{19}$$

$$E_{2\eta} = \frac{-\gamma}{hk_{2\zeta}^2}(-C_3 nF_{2n}(2ak_{2\zeta}e^{-\zeta}) + C_4\frac{j\omega\mu_2}{\gamma}2ak_{2\zeta}e^{-\zeta}G'_{2n}(2ak_{2\zeta}e^{-\zeta}))\sin(n\eta) \tag{20}$$

$$H_{1\zeta} = \frac{-\gamma}{hk_{1\zeta}^2}(-C_2 2ak_{1\zeta}e^{-\zeta}G'_{1n}(2ak_{1\zeta}e^{-\zeta}) + C_1\frac{nj\omega\varepsilon_1}{\gamma}F_{1n}(2ak_{1\zeta}e^{-\zeta}))\sin(n\eta) \tag{21}$$

$$H_{1\eta} = \frac{-\gamma}{hk_{1\zeta}^2}(C_2 nG_{1n}(2ak_{1\zeta}e^{-\zeta}) - C_1\frac{j\omega\varepsilon_1}{\gamma}2ak_{1\zeta}e^{-\zeta}F'_{1n}(2ak_{1\zeta}e^{-\zeta}))\cos(n\eta) \tag{22}$$

$$H_{2\zeta} = \frac{-\gamma}{hk_{2\zeta}^2}(-C_4 2ak_{2\zeta}e^{-\zeta}G'_{2n}(2ak_{2\zeta}e^{-\zeta}) + C_3\frac{nj\omega\varepsilon_2}{\gamma}F_{2n}(2ak_{2\zeta}e^{-\zeta}))\sin(n\eta) \tag{23}$$

$$H_{2\eta} = \frac{-\gamma}{hk_{2\zeta}^2}(C_4 nG_{2n}(2ak_{2\zeta}e^{-\zeta}) - C_3\frac{j\omega\varepsilon_2}{\gamma}2ak_{2\zeta}e^{-\zeta}F'_{2n}(2ak_{2\zeta}e^{-\zeta}))\cos(n\eta) \tag{24}$$

where

$$F'_{1n}(2ak_{1\zeta}e^{-\zeta}) = Y_n(2ak_{1\zeta}e^{-\zeta_1})J'_n(2ak_{1\zeta}e^{-\zeta}) - J_n(2ak_{1\zeta}e^{-\zeta_1})Y'_n(2ak_{1\zeta}e^{-\zeta}) \tag{25}$$

$$G'_{1n}(2ak_{1\zeta}e^{-\zeta}) = Y'_n(2ak_{1\zeta}e^{-\zeta_1})J'_n(2ak_{1\zeta}e^{-\zeta}) - J'_n(2ak_{1\zeta}e^{-\zeta_1})Y'_n(2ak_{1\zeta}e^{-\zeta}) \tag{26}$$

$$F'_{2n}(2ak_{2\zeta}e^{-\zeta}) = Y_n(2ak_{2\zeta}e^{-\zeta_3})J'_n(2ak_{2\zeta}e^{-\zeta}) - J_n(2ak_{2\zeta}e^{-\zeta_3})Y'_n(2ak_{2\zeta}e^{-\zeta}) \tag{27}$$

$$G'_{2n}(2ak_{2\zeta}e^{-\zeta}) = Y'_n(2ak_{2\zeta}e^{-\zeta_3})J'_n(2ak_{2\zeta}e^{-\zeta}) - J'_n(2ak_{2\zeta}e^{-\zeta_3})Y'_n(2ak_{2\zeta}e^{-\zeta}) \tag{28}$$

The continuity of the tangential electric- and magnetic-field components at $\zeta = \zeta_2$ relates the coefficients to one another as follows:

$$C_1 = C_3\frac{F_{2n}(2ak_{2\zeta}e^{-\zeta_2})}{F_{1n}(2ak_{1\zeta}e^{-\zeta_2})} \tag{29}$$

$$C_2 = C_4\frac{G_{2n}(2ak_{2\zeta}e^{-\zeta_2})}{G_{1n}(2ak_{1\zeta}e^{-\zeta_2})} \tag{30}$$

$$\frac{C_4}{C_3} = \frac{(\gamma n/2j\omega a e^{-\zeta_2})(1/k_{2\zeta}^2) - (1/k_{1\zeta}^2)}{(\mu_2/k_{2\zeta})(G'_{2n}(2ak_{2\zeta}e^{-\zeta_2})/F_{2n}(2ak_{2\zeta}e^{-\zeta_2})) - (\mu_1/k_{1\zeta})((G'_{1n}(2ak_{1\zeta}e^{-\zeta_2})G_{2n}(2ak_{2\zeta}e^{-\zeta_2}))/(G_{1n}(2ak_{1\zeta}e^{-\zeta_2})F_{2n}(2ak_{2\zeta}e^{-\zeta_2})))} \tag{31}$$

$$\frac{C_3}{C_4} = \frac{(\gamma n/2j\omega a e^{-\zeta_2})(1/k_{2\zeta}^2) - (1/k_{1\zeta}^2)}{(\varepsilon_2/k_{2\zeta})(F'_{2n}(2ak_{2\zeta}e^{-\zeta_2})/G_{2n}(2ak_{2\zeta}e^{-\zeta_2})) - (\varepsilon_1/k_{1\zeta})((F'_{1n}(2ak_{1\zeta}e^{-\zeta_2})F_{2n}(2ak_{2\zeta}e^{-\zeta_2}))/(F_{1n}(2ak_{1\zeta}e^{-\zeta_2})G_{2n}(2ak_{2\zeta}e^{-\zeta_2})))} \tag{32}$$

where (31) is used for HE modes and (32) is used for EH modes. Using (31) and (32), the coefficients C_3 and C_4 can be eliminated

https://doi.org/10.1017/S1759078720000926 Published online by Cambridge University Press

https://doi.org/10.1017/S1759078720000926 Published online by Cambridge University Press

Table 1. Cutoff wave numbers (k_{nm}) of the homogeneously filled eccentric coaxial cable (by considering $\varepsilon_{r1} = \varepsilon_{r2} = 1$)

	$D_2/R_1 = 0.04$, $R_3/R_1 = 0.448998$, $\zeta_1 = 25.79$, $\zeta_2 = 26.30$, $\zeta_3 = 26.59$				$D_2/R_1 = 0.05$, $R_3/R_1 = 0.05$, $\zeta_1 = 25.91$, $\zeta_2 = 26.42$, $\zeta_3 = 28.90$			
	Our method	CST	[15]	[9]	Our method	CST	[15]	[9]
TE_{11}	1.407452	1.406612	1.410028	1.403495	1.831567	1.828824	1.836132	1.821917
TE_{21}	2.765603	2.760412	2.771100	2.759585	3.053154	3.049438	3.061847	3.053905
TE_{31}	4.043847	4.041863	4.052665	4.038212	4.201182	4.195072	4.211770	4.201184
TE_{41}	5.242341	5.241353	5.254597	5.238405	5.317553	5.311384	5.330947	5.317553
TE_{51}	6.380165	6.371149	6.398096	6.380286	6.415616	6.413286	6.431776	6.415616
TM_{01}	5.657074	5.662340	5.680839	5.696181	3.064407	3.051532	3.072796	3.171976
TM_{11}	5.832915	5.843572	5.856573	5.869784	3.867325	3.876724	3.870190	3.888266
TM_{21}	6.327979	6.335568	6.351492	6.359170	5.136070	5.136550	5.149012	5.137403
TM_{31}	7.067177	7.059534	7.090828	7.091327	6.380166	6.380164	6.396237	6.380199
TM_{41}	7.971350	7.957891	7.995631	7.988750	7.588342	7.588316	7.607456	7.588343
	$D_2/R_1 = 0.2$, $R_3/R_1 = 0.3$, $\zeta_1 = 26.60$, $\zeta_2 = 27.11$, $\zeta_3 = 27.80$				$D_2/R_1 = 0.3$, $R_3/R_1 = 0.2$, $\zeta_1 = 26.80$, $\zeta_2 = 27.31$, $\zeta_3 = 28.41$			
	Our method	CST	[15]	[9]	Our method	CST	[15]	[9]
TE_{11}	1.582064	1.581393	1.645034	1.448657	1.705115	1.704489	1.863991	1.448657
TE_{21}	2.968501	2.958471	3.105751	2.824888	3.034724	3.022132	3.356513	2.824888
TE_{31}	4.180113	4.180977	4.388184	4.094783	4.199060	4.211983	4.656084	4.094783
TE_{41}	5.312973	5.310040	5.583345	5.274652	5.317342	5.309122	5.898109	5.274652
TE_{51}	6.414677	6.406139	6.742891	6.399644	6.415596	6.420103	7.116605	6.399644
TM_{01}	4.412394	4.413130	4.737715	5.095572	3.815956	3.827671	4.359074	5.288001
TM_{11}	4.705775	4.702137	5.031669	5.310905	4.235748	4.230319	4.790313	5.488033
TM_{21}	5.470236	5.469812	5.805374	5.902924	5.221768	5.208912	5.831205	6.043230
TM_{31}	6.493723	6.481075	6.854954	6.756020	6.394599	6.371992	7.104403	6.854501
TM_{41}	7.622847	7.606661	8.025803	7.762377	7.590375	7.581112	8.422163	7.824947

Comparison with [9], [15] and simulation results ($R_2/R_1 = 0.6$, $D_1/R_1 = 10^{-24}$).

Table 2. Cutoff frequencies (GHz) of the dielectric-lined eccentric coaxial cable

	$R_2/R_1 = 0.9$, $R_3/R_1 = 0.4$, $D_1/R_1 = 0.0001$, $D_2/R_1 = 0.1$, $\varepsilon_{r1} = 3.6$, $\varepsilon_{r2} = 1$		$R_2/R_1 = 0.9$, $R_3/R_1 = 0.4$, $D_1/R_1 = 0.0001$, $D_2/R_1 = 0.2$, $\varepsilon_{r1} = 3.6$, $\varepsilon_{r2} = 1$		$R_2/R_1 = 0.9$, $R_3/R_1 = 0.4$, $D_1/R_1 = 0.0001$, $D_2/R_1 = 0.3$, $\varepsilon_{r1} = 3.6$, $\varepsilon_{r2} = 1$	
	Our method	CST	Our method	CST	Our method	CST
TE_{01}	248.198675	248.197915	247.096590	247.095211	246.732155	246.733176
TE_{02}	299.730863	299.729967	298.657998	298.656734	298.303595	298.301603
TE_{03}	434.862931	434.856042	432.694971	432.693411	431.978574	431.962311
TM_{01}	176.006973	176.005897	175.434797	175.429566	175.245768	175.241153
TM_{02}	239.144539	239.143188	238.047570	238.042201	237.684862	237.670322
TM_{03}	430.499821	430.497565	428.327311	428.315003	427.609382	427.621331
HE_{11}	66.667619	66.666960	66.525358	66.524134	66.478223	66.476388
HE_{21}	127.054575	127.053312	126.728092	126.717440	126.619862	126.610121
HE_{31}	177.804806	177.798117	177.255854	177.240131	177.073878	177.061550
EH_{11}	197.439355	197.425745	196.881589	196.867514	196.697326	196.714411
EH_{21}	250.052293	250.043810	249.492465	249.463892	249.307472	249.313655
EH_{31}	307.431157	307.421777	306.218550	306.205032	305.817175	305.802249
	$R_2/R_1 = 0.45$, $R_3/R_1 = 0.3$, $D_1/R_1 = 0.1$, $D_2/R_1 = 0.0001$, $\varepsilon_{r1} = 1$, $\varepsilon_{r2} = 3.6$		$R_2/R_1 = 0.55$, $R_3/R_1 = 0.3$, $D_1/R_1 = 0.2$, $D_2/R_1 = 0.0001$, $\varepsilon_{r1} = 1$, $\varepsilon_{r2} = 3.6$		$R_2/R_1 = 0.65$, $R_3/R_1 = 0.3$, $D_1/R_1 = 0.3$, $D_2/R_1 = 0.0001$, $\varepsilon_{r1} = 1$, $\varepsilon_{r2} = 3.6$	
	Our method	CST	Our method	CST	Our method	CST
TE_{01}	205.857315	205.856670	169.308884	169.306771	143.447910	143.445932
TE_{02}	347.503081	347.502899	314.886285	314.871440	224.286718	224.275340
TE_{03}	526.208343	526.206323	331.878215	331.863113	313.314054	313.305433
TM_{01}	192.411708	192.409111	158.202830	158.217551	130.841839	130.830243
TM_{02}	285.569962	285.552203	177.833569	177.827604	134.043939	134.027562
TM_{03}	341.349842	341.329440	325.977151	325.957339	307.795175	307.779605
HE_{11}	67.241616	67.242353	61.879409	61.878145	56.811218	56.801424
HE_{21}	132.316790	132.301211	123.161193	123.153979	113.230701	113.228084
HE_{31}	193.598966	193.582232	183.286062	183.274211	169.037847	169.023211
EH_{11}	205.857315	205.846735	169.308884	169.319486	143.447910	143.431398
EH_{21}	241.510679	241.522107	198.808248	198.791109	168.418962	168.399511
EH_{31}	290.727796	290.719899	239.691188	239.671290	203.010208	203.029704

Comparison with simulation results.

to obtain the following dispersion relation:

$$QV = \left(\frac{\gamma n}{2\omega a e^{-\zeta_2}}\right)^2 \left(\frac{1}{k_{2\zeta}^2} - \frac{1}{k_{1\zeta}^2}\right)^2 \tag{33}$$

where

$$Q = \frac{\mu_2}{k_{2\zeta}} \frac{G'_{2n}(2ak_{2\zeta}e^{-\zeta_2})}{F_{2n}(2ak_{2\zeta}e^{-\zeta_2})} - \frac{\mu_1}{k_{1\zeta}} \frac{G'_{1n}(2ak_{1\zeta}e^{-\zeta_2})G_{2n}(2ak_{2\zeta}e^{-\zeta_2})}{G_{1n}(2ak_{1\zeta}e^{-\zeta_2})F_{2n}(2ak_{2\zeta}e^{-\zeta_2})} \tag{34}$$

$$V = \frac{\varepsilon_2}{k_{2\zeta}} \frac{F'_{2n}(2ak_{2\zeta}e^{-\zeta_2})}{G_{2n}(2ak_{2\zeta}e^{-\zeta_2})} - \frac{\varepsilon_1}{k_{1\zeta}} \frac{F'_{1n}(2ak_{1\zeta}e^{-\zeta_2})F_{2n}(2ak_{2\zeta}e^{-\zeta_2})}{F_{1n}(2ak_{1\zeta}e^{-\zeta_2})G_{2n}(2ak_{2\zeta}e^{-\zeta_2})} \tag{35}$$

The characteristic equations of TE_{0m} and TM_{0m} modes can be obtained by setting $n = 0$ in (33) as follows:

$$F_{20}(2ak_{2\zeta}e^{-\zeta_2})(\mu_2 k_{1\zeta} G'_{20}(2ak_{2\zeta}e^{-\zeta_2})G_{10}(2ak_{1\zeta}e^{-\zeta_2}) - \mu_1 k_{2\zeta} G'_{10}(2ak_{1\zeta}e^{-\zeta_2})G_{20}(2ak_{2\zeta}e^{-\zeta_2})) = 0 \tag{36}$$

$$G_{20}(2ak_{2\zeta}e^{-\zeta_2})(\varepsilon_2 k_{1\zeta} F'_{20}(2ak_{2\zeta}e^{-\zeta_2})F_{10}(2ak_{1\zeta}e^{-\zeta_2}) - \varepsilon_1 k_{2\zeta} F'_{10}(2ak_{1\zeta}e^{-\zeta_2})F_{20}(2ak_{2\zeta}e^{-\zeta_2})) = 0 \tag{37}$$

where the roots of (36) and (37) represent the cutoff frequencies of the TE_{0m} and TM_{0m} modes, respectively.

For hybrid modes ($n \neq 0$ and at cutoff ($\gamma = 0$)), the right-hand side of the dispersion relation (33) becomes zero and the HE and

https://doi.org/10.1017/S1759078720000926 Published online by Cambridge University Press

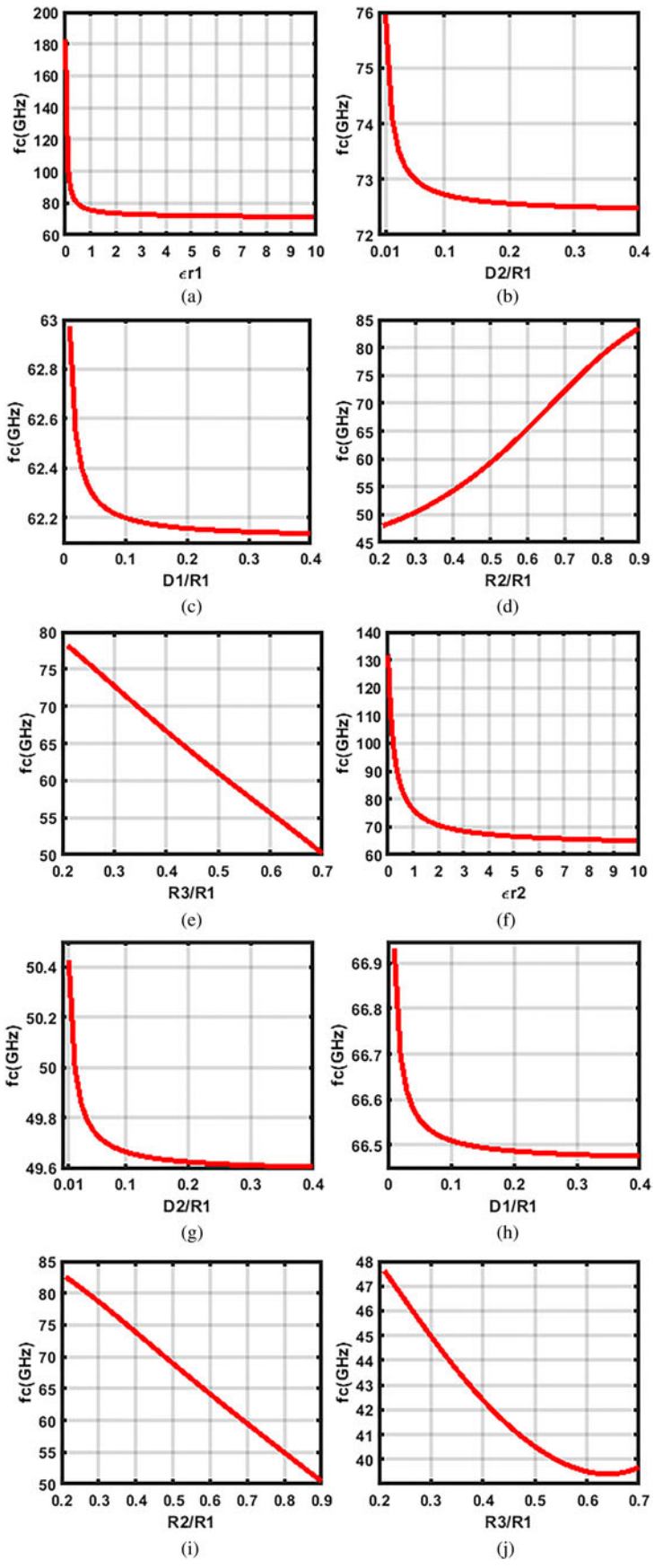


Fig. 2. HE_{11}-mode cutoff frequency versus the different physical and geometrical parameters of the problem. (a) ε_{r1} ($D_2/R_1 = 0.2$, $D_1/R_1 = 0.0001$, $R_2/R_1 = 0.9$, $R_3/R_1 = 0.3$, $\varepsilon_{r2} = 1$), (b) D_2 ($D_1/R_1 = 0.0001$, $R_2/R_1 = 0.9$, $R_3/R_1 = 0.3$, $\varepsilon_{r1} = 3.6$, $\varepsilon_{r2} = 1$), (c) D_1 ($D_2/R_1 = 0.0001$, $R_2/R_1 = 0.55$, $R_3/R_1 = 0.1$, $\varepsilon_{r1} = 3.6$, $\varepsilon_{r2} = 1$), (d) R_2 ($D_1/R_1 = 0.0001$, $D_2/R_1 = 0.1$, $R_3/R_1 = 0.1$, $\varepsilon_{r1} = 3.6$, $\varepsilon_{r2} = 1$), (e) R_3 ($D_1/R_1 = 0.0001$, $D_2/R_1 = 0.1$, $R_2/R_1 = 0.9$, $\varepsilon_{r1} = 3.6$, $\varepsilon_{r2} = 1$), (f) ε_{r2}($D_2/R_1 = 0.01$, $D_1/R_1 = 0.0001$, $R_2/R_1 = 0.45$, $R_3/R_1 = 0.3$, $\varepsilon_{r1} = 1$), (g) D_2 ($D_1/R_1 = 0.0001$, $R_2/R_1 = 0.8$, $R_3/R_1 = 0.3$, $\varepsilon_{r1} = 1$, $\varepsilon_{r2} = 3.6$), (h) D_1 ($D_2/R_1 = 0.0001$, $R_2/R_1 = 0.55$, $R_3/R_1 = 0.1$, $\varepsilon_{r1} = 1$, $\varepsilon_{r2} = 3.6$), (i) R_2 ($D_1/R_1 = 0.0001$, $D_2/R_1 = 0.1$, $R_3/R_1 = 0.1$, $\varepsilon_{r1} = 1$, $\varepsilon_{r2} = 3.6$), (j) R_3 ($D_1/R_1 = 0.0001$, $D_2/R_1 = 0.1$, $R_2/R_1 = 0.9$, $\varepsilon_{r1} = 1$, $\varepsilon_{r2} = 3.6$).

https://doi.org/10.1017/S1759078720000926 Published online by Cambridge University Press

EH modes are decoupled. This results in the following characteristic equations for hybrid modes:

$$F_{2n}(2ak_{2\zeta}e^{-\zeta_2})(\mu_2 k_{1\zeta}G'_{2n}(2ak_{2\zeta}e^{-\zeta_2})G_{1n}(2ak_{1\zeta}e^{-\zeta_2}) - \mu_1 k_{2\zeta}G'_{1n}(2ak_{1\zeta}e^{-\zeta_2})G_{2n}(2ak_{2\zeta}e^{-\zeta_2})) = 0, \quad n \neq 0 \tag{38}$$

$$G_{2n}(2ak_{2\zeta}e^{-\zeta_2})(\varepsilon_2 k_{1\zeta}F'_{2n}(2ak_{2\zeta}e^{-\zeta_2})F_{1n}(2ak_{1\zeta}e^{-\zeta_2}) - \varepsilon_1 k_{2\zeta}F'_{1n}(2ak_{1\zeta}e^{-\zeta_2})F_{2n}(2ak_{2\zeta}e^{-\zeta_2})) = 0, \quad n \neq 0 \tag{39}$$

where the roots of (38) and (39) represent the cutoff frequencies of the HE and EH modes, respectively.

Results and discussion

To check the accuracy of the calculations, two special cases have been investigated. The first corresponds to partially filled coaxial cable. To achieve this, D_1, $D_2 \to 0$ must be considered. The cutoff frequencies can be calculated for different values of R_1, R_2, and R_3. For these calculations, we can put $D_1/R_1 = 10^{-10}$ and $D_2/R_1 = 10^{-15}$. Comparison with the exact results reported in [19] gives agreement to seven significant digits. The second case is related to a homogeneously filled eccentric coaxial cable, where the fields inside the region are either TE or TM. Such a case can be achieved by considering $\varepsilon_1 = \varepsilon_2 = \varepsilon$. In [15], it was mentioned that the solution is valid for $D_2/R_1 \leq 0.05$. However, in this study, we can obtain the results for any arbitrary values of D_2/R_1 in homogeneously filled eccentric coaxial cable (by considering $\varepsilon_1 = \varepsilon_2 = \varepsilon$). Because, there are more parameters in the analysis of a partially filled eccentric coaxial cable than a homogeneously filled eccentric coaxial cable which can satisfy the main limiting condition in BCS ($\cosh(\zeta) \gg 1$ or $|\zeta| \geq 3$), without limiting the values for D_2/R_1. In other words, we can keep D_1/R_1 negligible instead of D_2/R_1 so that the values of ζ remain larger than 3. To show this, in Table 1, the cutoff wavenumbers (k_{nm}) of the homogeneously filled eccentric coaxial cable are calculated for several different values of D_2/R_1 and R_3/R_1 using our method, and the results are compared with those given in [9] and [15], and also their simulation values. For these calculation we put $D_1/R_1 = 10^{-24}$. Full-wave frequency-domain simulations (using CST Microwave Studio) have been used for the calculations, where 6 743 881 elements in the mesh were used. As it can be found from Table 1, one of the substantial features of our method is that it remains valid even for larger values of D_2/R_1, where the methods used in [9] and [15] have shown a significant weakness. It is noteworthy to mention again that the limiting condition for the method used in [15] is $D_2/R_1 = 1$. Moreover, the method used in [9] is based on transforming eccentric coaxial into coaxial configuration using bilinear transformation expressed in terms of mutually inverse points and gives acceptable results as long as the values of ρ_1'/R_3 and ρ_2'/R_3 are negligible, where ρ_1' and ρ_2' are the radius of the inner and outer cylinders of the transformed coaxial configuration, respectively. However, as D_2/R_1 increases the values of ρ_1' and ρ_2' become comparable with R_3, which brings about large errors in the final results for large values of D_2/R_1.

In Table 2, the cutoff frequencies of a dielectric-lined eccentric coaxial cable are calculated for a number of the higher order modes (TE, TM, HE, and EH) using our method, and the results are compared with their simulation values. The good agreement between the data justifies the validity of the analysis. Figure 2 illustrates the variations of the cutoff frequencies of HE_{11}-mode versus the different physical and geometrical parameters of the problem, where in Figs 2(a)–(e), the liner is considered to be on the outer conductor ($\varepsilon_{r2} = 1$), and in Figs 2(f)–2(j) it is put on the inner conductor ($\varepsilon_{r1} = 1$). As one can see, for the both cases, even though the dielectric liner only occupies a small portion of the total cross-section of the waveguide, it is to be expected that a thin epsilon-positive liner with permittivity larger than unity slightly lowers the natural cutoff frequency, and reversely, that an epsilon-positive liner with permittivity smaller than unity will increase it. In other words, the cutoff frequency is to a low extent dependent on large positive permittivity values whereas it increases significantly for small ones, suggesting that the waveguide is thrust more deeply into cutoff as the liner permittivity is positive and tending to zero (Figs 2(a) and 2(f)). Besides, the cutoff frequency is to a high extent dependent on small eccentricities (D_1/R_1, $D_2/R_1 < 0.05$) while it almost remains stable for larger ones (Figs 2(b), 2(c), 2(g) and 2(h)). It is noteworthy to mention that the variation of eccentricity has its maximum effect on the cutoff frequency when the liner is on the outer conductor and D_2/R_1 is changing (Fig. 2(b)). Moreover, the cutoff frequency can be decreased by considering either thicker liner (Figs 2(d) and 2(i)) or the inner conductor with larger radius (Figs 2(e) and 2(j)). It should be mentioned that in Fig. 2(j), we see gradual decline in cutoff frequency, because as R_3/R_1 increases, the liner thickness decreases accordingly. Figure 2 may be employed in choosing the value of permittivity and dimensions required to achieve a desired cutoff frequency of HE_{11} mode in a partially filled eccentric coaxial cable.

Conclusion

The problem has been investigated in a fully analytical manner and the analytical expressions have been obtained for the electric and magnetic field functions and the cutoff frequencies. The presented method gives accurate results for either $D_1/R_1 = 1$ and every arbitrary value of D_2/R_1, or $D_2/R_1 = 1$ and every arbitrary value of D_1/R_1. An excellent agreement has been observed between the calculated cutoff frequencies with those obtained by full-wave simulations. The combination of accuracy, analyticity and ease of implementation makes this method an appropriate candidate for the analysis of eccentric coaxial line structures. Moreover, it has been shown this method significantly works better than the method presented in [15] in calculating the cut off frequencies of a homogeneously filled eccentric circular metallic waveguide.

References

1. **Chakrabarty SB, Sharma SB and Das BN** (2009) Higher-order modes in circular eccentric waveguides. *Electromagnetics* **29**, 377–383.
2. **Davidovitz M and Lo YT** (1987) Cutoff wavenumbers and modes for annular-cross-section waveguide with eccentric inner conductor of small radius. *IEEE Transactions on Microwave Theory and Techniques* **35**, 510–515.
3. **Kotsis AD and Roumeliotis JA** (2014) Cutoff wavenumbers of eccentric circular metallic waveguides. *IET Microwaves, Antennas & Propagation* **8**, 104–111.
4. **Kotsis AD and Roumeliotis JA** (2017) Cutoff wavenumbers of circular metallic waveguides with eccentricity. *Proceedings of 19th Conference Computation of Electromagnetic Fields (COMPUMAG)*. pp. 1–2.
5. **Yee HY and Audeh NF** (1966) Cutoff frequencies of eccentric waveguides. *IEEE Transactions on Microwave Theory and Techniques* **14**, 487–493.

https://doi.org/10.1017/S1759078720000926 Published online by Cambridge University Press

6. **Abaka E** (1969) TE and TM modes in transmission lines with circular outer conductor and eccentric circular inner conductor. *Electronics Letters* **5**, 251–252.
7. **Roumeliotis JA, Hossain AS and Fikioris JG** (1980) Cutoff wave numbers of eccentric circular and concentric circular-elliptic metallic wave guides. *Radio Science* **15**, 923–937.
8. **Kuttler JR** (1984) A new method for calculating TE and TM cutoff frequencies of uniform waveguides with lunar or eccentric annular cross section. *IEEE Transactions on Microwave Theory and Techniques* **32**, 348–354.
9. **Das BN and Vargheese OJ** (1994) Analysis of dominant and higher order modes for transmission lines using parallel cylinders. *IEEE Transactions on Microwave Theory and Techniques* **42**, 681–683.
10. **Lin SL, Li LW, Yeo TS and Leong MS** (2001) Analysis of metallic waveguides of a large class of cross sections using polynomial approximation and superquadric functions. *IEEE Transactions on Microwave Theory and Techniques* **49**, 1136–1139.
11. **Yang H and Lee S** (2001) A variational calculation of TE and TM cutoff wavenumbers in circular eccentric guides by conformal mapping. *Microwave and Optical Technology Letters* **31**, 381–384.
12. **Das BN and Chakrabarty SB** (1995) Evaluation of cut-off frequencies of higher order modes in eccentric coaxial line. *IEE Proceedings-Microwaves, Antennas and Propagation* **142**, 350–356,.
13. **Das BN, Chakrabarty SB and Mallick AK** (1995) Cutoff frequencies of guiding structures with circular and planar boundaries. *IEEE Microwave and Guided Wave Letters* **5**, 186–188, .
14. **Fan CM, Young DL and Chiu CL** (2009) Method of fundamental solutions with external source for the eigenfrequencies of waveguides. *Journal of Marine Science and Technology* **17**, 164–172.
15. **Gholizadeh M, Baharian M and Kashani FH** (2019) A simple analysis for obtaining cutoff wavenumbers of an eccentric circular metallic waveguide in bipolar coordinate system. *IEEE Transactions on Microwave Theory and Techniques* **67**, 837–844.
16. **Dey R, Agnihotri I, Chakrabarty S and Sharma SB** (2007) Cut-off wave number and dispersion characteristics of eccentric annular guide with dielectric support. In *2007 IEEE Applied Electromagnetics Conference (AEMC)*. December 2007, pp. 1–4.
17. **Vardiambasis IO, Tsalamengas JL and Kostogiannis K** (2003) Propagation of EM waves in composite bianisotropic cylindrical structures. *IEEE Transactions on Microwave Theory and Techniques* **51**, 761–766.
18. **Gholizadeh M and Hojjat-Kashani F** (2020) A new analytical method for studying higher order modes of a two-wire transmission line. *Progress in Electromagnetics Research* **88**, 11–20.
19. **Lewis JE and Kharadly MMZ** (1968) Surface-wave modes in dielectric-lined coaxial cables. *Radio Science* **3**, 1167–1174.



M. Gholizadeh was born in Ahvaz, Iran, in 1991. He received a degree in electrical engineering from the Faculty of Engineering, Shahid Chamran University, Ahvaz, in 2015. He is currently pursuing his master's degree in electrical engineering-fields and waves at the Iran University of Science and Technology, Tehran, Iran. His current research interests include fundamental electromagnetic theory, electromagnetic waves propagation, electromagnetic scattering, microwave circuits, microwave transmission lines, and cavities.



F. H. Kashani was born in Mashhad, Iran, in 1941. He received his bachelor's degree in electrical engineering from the Faculty of Engineering, University of Tehran, Tehran, Iran, in 1963, and his master's and Ph.D. degrees in electronics from the University of California at Los Angeles (UCLA), Los Angeles, CA, USA, in 1969 and 1971, respectively. He is currently a Professor of electrical engineering with the Iran University of Science and Technology, Tehran. His master's and Ph.D. research area was dispersion of waves and measuring the picosecond waves. He has taught telecommunication courses at UCLA and The University of Sydney, Sydney, NSW, Australia, for some time. After returning to Iran, he has spent many years teaching the undergraduate, postgraduate, and Ph.D. courses at the Sharif University of Technology, Tehran, University of Science and Technology, and Islamic Azad University, Tehran. He has also supervised many students in telecommunications and electronics.

https://doi.org/10.1017/S1759078720000926 Published online by Cambridge University Press